

Experimental investigation of CO₂ capture using sodium hydroxide particles in a fluidized bed

Sareh Naeem, Ahad Ghaemi[†], and Shahrokh Shahhosseini

School of Chemical Engineering, Iran University of Science and Technology (IUST), Tehran, Iran

(Received 27 June 2015 • accepted 8 November 2015)

Abstract—CO₂ capture from air using sodium hydroxide solid sorbent in a laboratory scale fluidized bed reactor was investigated experimentally. The influence of three parameters of temperature, inlet CO₂ volume percentage and inlet air flow rate on the CO₂ removal rate was studied. Experimental results showed that the optimum rate was at 25 °C when the inlet CO₂ volume percentage was 1%. The results also showed that the adsorption process was reactive, and the reaction mechanism depended on the reaction temperature. In addition, empirical observation revealed only one adsorption cycle happened at low temperatures (25-30 °C). As the temperature increased, the second adsorption cycle occurred and, finally, CO₂ desorption cycle took place in the range of 90-115 °C.

Keywords: Adsorption, CO₂ Capture, Fluidized Bed Reactor, Sodium Hydroxide

INTRODUCTION

CO₂ capture using diverse sorbents has been one of the most popular fields of research in recent years. Absorption using amine solutions is the most popular commercial method to separate carbon dioxide [1,2]. However, this technique has some disadvantages such as high energy consumption for solvent recovery, wide corrosion of the apparatus, loss of the solvent via evaporation and accelerated degradation of the solvent in the presence of oxygen [3-5].

Lately, CO₂ chemical adsorption using regenerable solid sorbents has been investigated as an innovative method [6-13]. In this method, CO₂ is efficiently removed from the gas flow due to its reaction with a solid sorbent. Using solid sorbents has some advantages, including high capacity of the chemical adsorption, low thermal capacity, the possibility of producing pure carbon dioxide and environmental advantages [6,14-21].

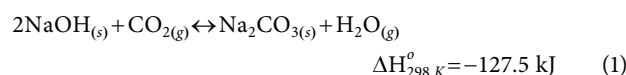
Heat control is required to prevent the formation of hot spots during the extremely exothermic adsorption reaction in the solid sorbent process. Fluidized bed reactors can be the best option for CO₂ capture by solid sorbents, which has efficient heat and mass transfer owing to the high contact surface between the gas and solid sorbent. Also, fluidized bed reactors prevent the formation of hot zones by making near isothermal conditions due to fast circulation of the particles in the reactor [22-24].

Several processes for CO₂ capture from air can be found in the literature. Zhang et al. [25] developed PEI-silica adsorbent for CO₂ capture from ambient air in a bubbling fluidized bed reactor. Kianpour et al. [7] experimentally investigated CO₂ capture by carbonation of NaOH in a batch reactor and studied the influence of various operating parameters on the CO₂ removal rate. Nikulshina et al. [14] suggested a thermochemical cyclic process for the continu-

ous removal of CO₂ from ambient air in a fluidized bed solar reactor with consecutive CaO-carbonation and CaCO₃-calcination steps. Nikulshina et al. [26] examined the thermodynamics and kinetics of the pertinent reactions for three selected Na-based closed-material cycles for CO₂ capture from air. Thermogravimetric runs were made at low CO₂ concentration (500 ppm) to simulate the capture of CO₂ from air.

Based on the authors' best knowledge, there is no comprehensive study on CO₂ capture from air using solid sodium hydroxide in a fluidized bed. Therefore, we investigated the effect of operating parameters on CO₂ capture.

We experimentally investigated low temperature (25-40 °C) CO₂ sorption from ambient air of mines and beverage production plants [27] using sodium hydroxide (NaOH) particles in a fluidized bed reactor. For centuries, miners have been aware of the occupational hazard of "black damp," a condition of low oxygen levels in mine shafts. It was common for miners to send a candle or mouse into the mine prior to entering and to watch for the candle to extinguish or the mouse to lose consciousness, indicating a lack of oxygen, hence, a poor working environment. Brewers also are confronted with the potential of CO₂ poisoning. Yeast releases CO₂ as a byproduct in the process of fermenting alcohol. A study determined that they are exposed to 1.08% of CO₂ over an 8-hour workday on average [27]. Nikulshina et al. [26] proposed the following two reactions (thermodynamic cycles) for CO₂ sorption using sodium hydroxide:



where the forward and the backward reactions represent the carbonation and the calcination steps, respectively.

Moreover, in this study the optimal conditions for carbon dioxide capture in a fluidized bed using dry NaOH and the effects of

[†]To whom correspondence should be addressed.

E-mail: aghaemi@iust.ac.ir

Copyright by The Korean Institute of Chemical Engineers.

Table 1. Chemical composition of the sorbent

| Chemical component | Weight percent |
|---------------------------------|----------------|
| Sodium hydroxide NaOH | 98% wt min |
| NaCl | 0.022% wt max |
| Na ₂ CO ₃ | 0.94% wt max |
| Na ₂ SO ₄ | 1.038% wt max |
| Fe | 5 ppm wt max |
| Ni pick up | 3 ppm wt max |

operating parameters have also been investigated.

MATERIALS AND METHODS

Sodium hydroxide was chosen as sorbent due to its ability to adsorb CO₂ at ambient temperature with fast kinetics and affordable price. CO₂ gas (Sabalan Gas Co., Iran) and NaOH (Rita Chemical Raw Material Co., Saudi Arabia) were used for all the experiments with purities of 99.9% and 98%, respectively. Chemical composition of sorbent is indicated in Table 1.

Shape, bulk density, size, and sorbent particles size distribution are the key parameters in evaluating fluidization and solid circulation in a fluidized bed process. Chosen bulk density of the sorbent (1.175 g/ml) was in the recommended range, which is normally used in fluidized bed processes (higher than 0.8 g/ml) [28]. Size distribution of the sorbent spherical particles was within the range of 500–700 μm with a mean size of 600 μm and density of 2,130 kg/m³.

1. Experimental Setup and Procedure

Fig. 1 is a schematic illustration of the fluidized bed experimental setup. It is consisted of a Pyrex cylinder of 0.07 m in diameter and 0.5 m in height. Flow rate of the mixture of air and carbon

dioxide was measured with rotameters (Azmoon Motamam Co., Tehran, Iran), which were scaled based on the air density at 1 atm and 20 °C, i.e., 1.2045 kg/m³. Then, the mixture was injected into the inlet of the bed via a gas distributor. Afterwards, 0.1 kg of the sorbent was added to the reactor and CO₂ content of the inlet gas flow was adsorbed by NaOH solid sorbent. The gas mixture was heated by using a heating element (1 kW), of which the control temperature was between 25 to 40 °C. The temperatures were measured by the thermocouples embedded inside the body of the reactor at different parts of the bed. CO₂ concentration of the outlet gas flow was determined continuously using a standard gas analyzer at the exit of the bed.

In the usual procedure of fluidizing solid sorbent particles in a fluidized bed, the particles are first added to the bed, and then the gas is blown to fluidize the bed. In the case of sodium hydroxide, particles adsorb ambient moisture immediately after entering the bed and become sticky, therefore, making fluidization impossible. For this reason, in this study, first the gas flow was run through the bed and then the particles were added.

2. Analysis Methods

A gas analyzer, Testo-327-1 sensor (Testo, Germany), was calibrated and used for online CO₂ monitoring at the outlet of the fluidized bed. Resolutions of this instrument for CO₂ volume percentage and temperature were 0.01% and 0.1 °C, respectively. Recording temperature was every 0.3 s using temperature sensors (transmitter type TM-1230) embedded in the reactor. Resolution and response time of the temperature sensors were 0.5 °C and 5–30 s, respectively.

3. Design of the Experiments

Temperature, CO₂ volume percentage, and air flow rate at three different levels were considered as the main operating parameters. Nine experiments were designed to find the optimum experimental conditions, which are displayed in Table 2. To ensure the repeatability of the results, the experiments were performed at least twice

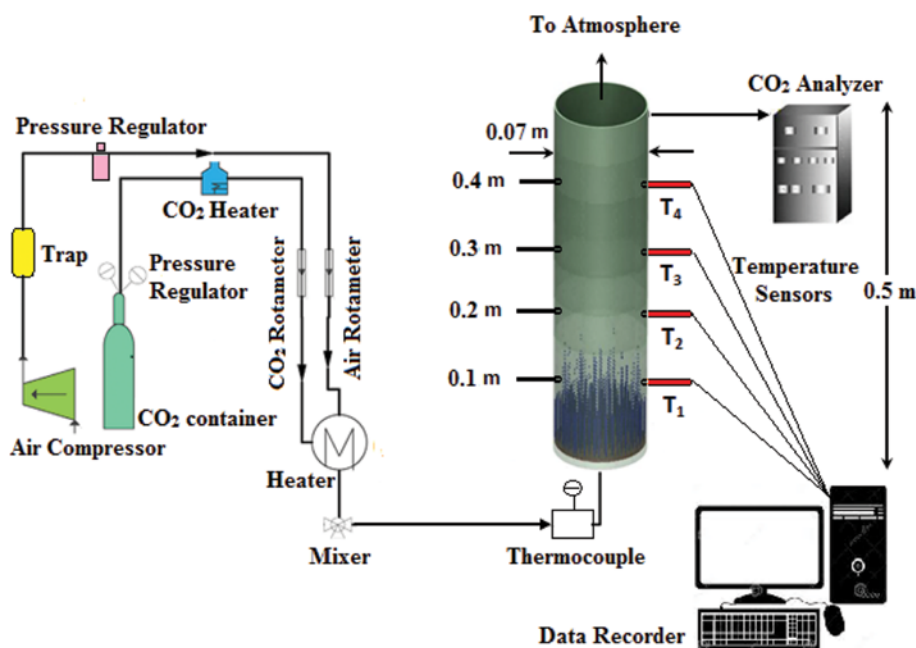


Fig. 1. A schematic representation of the laboratory experimental setup.

Table 2. Suggested design of the experiments and its result

| Run | Temperature (°C) | %CO ₂ | Air flow rate Q (m ³ /hr) | $\Delta C/\Delta t$ (%/s) | $\Delta C/\Delta t$ (ppm/s) |
|-----|------------------|------------------|--------------------------------------|---------------------------|-----------------------------|
| 1 | 25 | 1.0 | 14 | 0.0515 | 515.2777 |
| 2 | 25 | 1.5 | 15 | 0.0263 | 263.9534 |
| 3 | 25 | 2.0 | 16 | 0.0118 | 118.7500 |
| 4 | 30 | 1.0 | 15 | 0.0285 | 285.7142 |
| 5 | 30 | 1.5 | 16 | 0.0257 | 257.5757 |
| 6 | 30 | 2.0 | 14 | 0.0140 | 140.9090 |
| 7 | 40 | 1.0 | 16 | 0.0085 | 85.6353 |
| 8 | 40 | 1.5 | 14 | 0.0156 | 156.9230 |
| 9 | 40 | 2.0 | 15 | 0.0122 | 122.2222 |

and the average values were reported.

4. Sorbent Characteristics

Powder X-ray diffraction (XRD) characterization of NaOH samples was conducted prior to and after CO₂ sorption using an STOE STADI-MP (Germany) X-ray diffractometer with Cu-K α radiation. The accelerating voltage and the applied current were 40 kV

and 30 mA, respectively. The XRD patterns were recorded over a 2θ range between 5° and 90°. The results are displayed in Fig. 2.

RESULTS AND DISCUSSION

1. Determination of the Minimum Fluidization Flow Rate

NaOH sorbent falls into the group-B powders according to Geldart's fluidization classification [29]. To specify the minimum fluidization flow rate, ΔP (pressure difference) was measured against air flow rate at ambient temperature. A linear relation was observed while the bed was static, and there was a constant trend regardless of further increase in the air flow rate when the bed was being fluidized. According to the results of experiments, a flow rate of about 12 m³/hr was considered as the transition point and the minimum rate required for fluidization. To ensure being in the bubbling fluidization regime, an air flow rate was kept to 14 m³/hr during the adsorption tests.

2. Adsorption Analysis

To ensure a steady state process, the desired bed conditions were kept constant for around 50 s. Then, 0.1 kg of sodium hydroxide sorbent was added to the bed. During the initial seconds, a slight

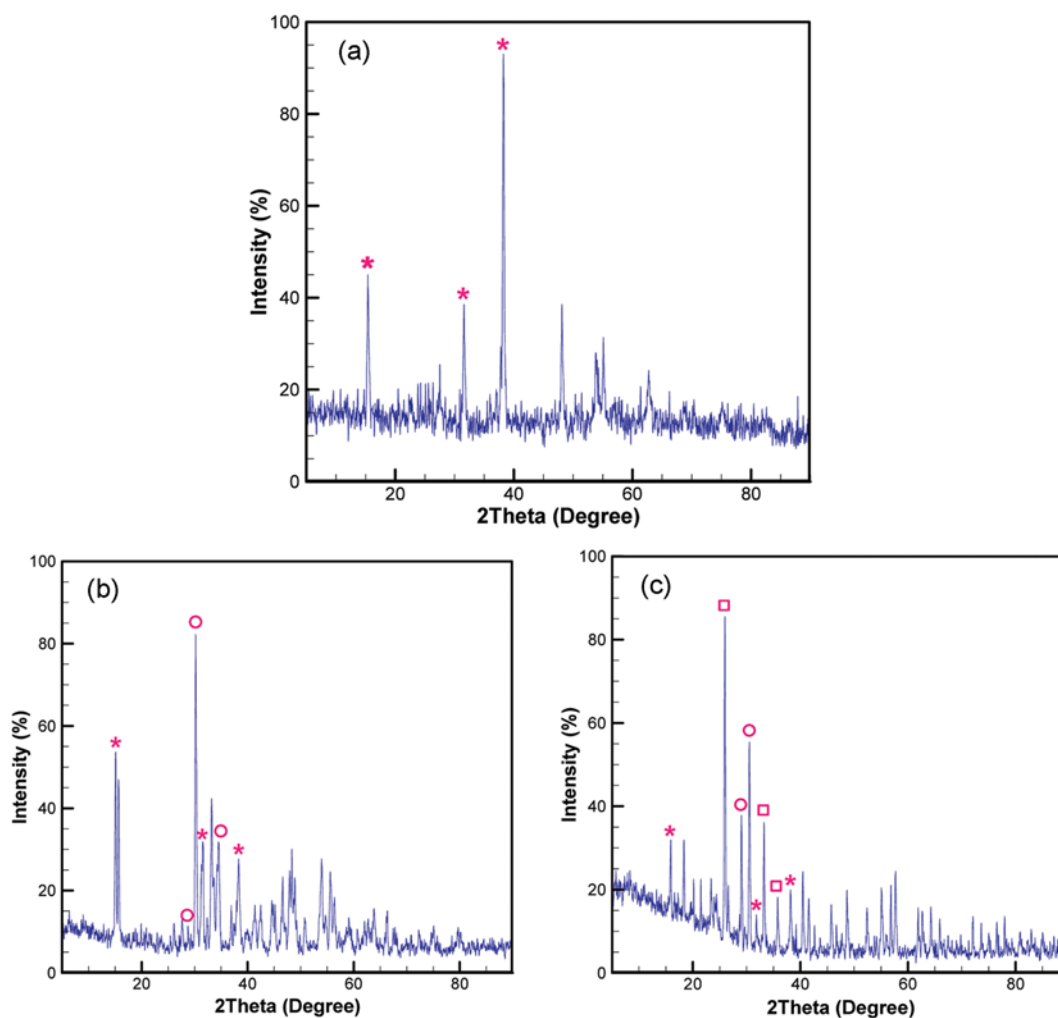


Fig. 2. Sorbent XRD analysis (a) fresh (b) run 1 in Table 2 (one adsorption cycle) (c) run 9 in Table 2 (two adsorption cycles), *: NaOH, □: Na₂CO₃, O: NaHCO₃.

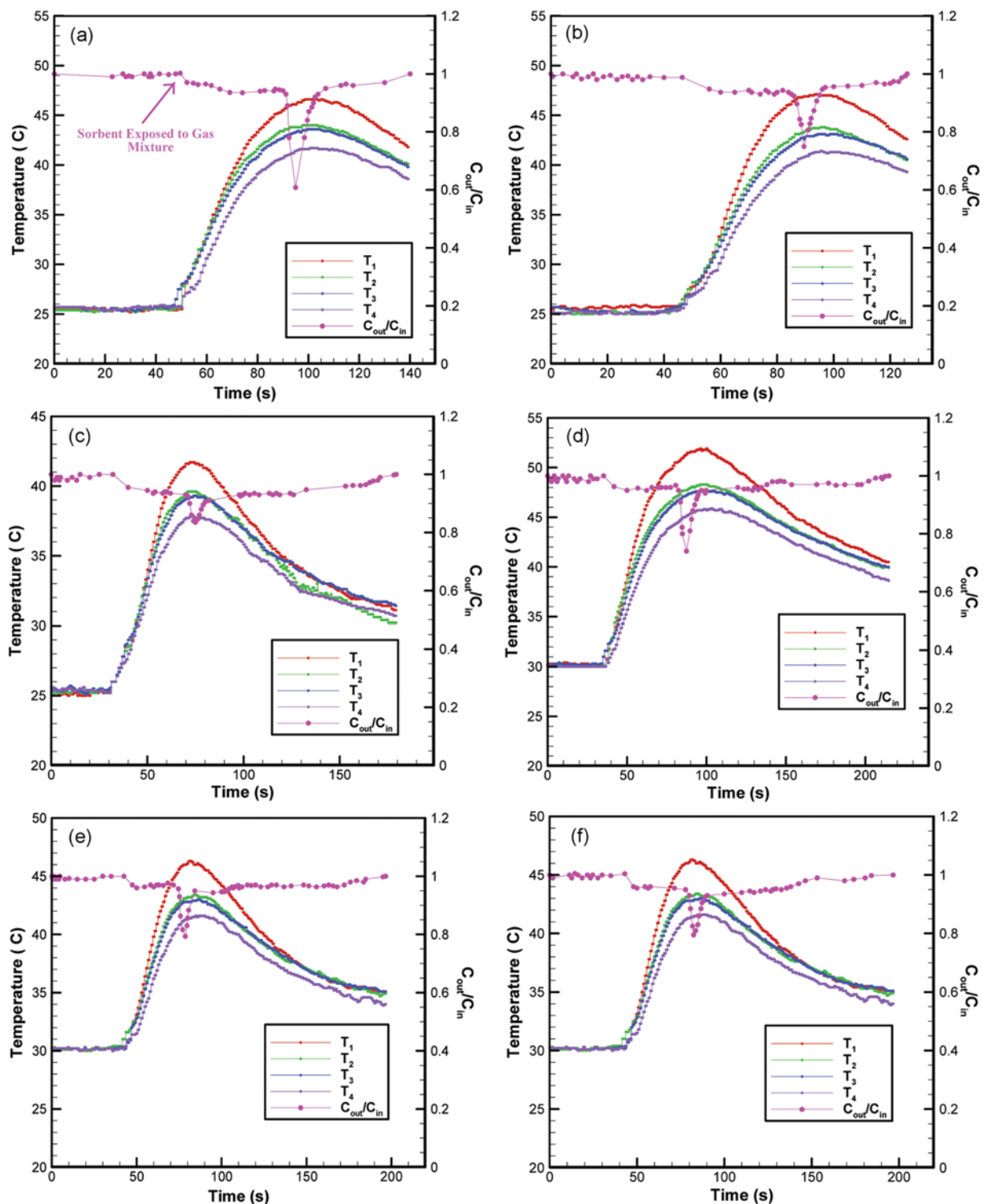


Fig. 3. The result of runs 1-6 of Table 2.

decrease in the ratio of output to input concentration of carbon dioxide (C_{out}/C_{in}) was observed, but over time, this ratio was reduced significantly, and at the same time the temperatures along the bed height increased remarkably. This confirms the exothermic nature of the chemical reactions, and reveals that chemisorption occurred in this process. The results of the designed experiments (Table 2)

are presented in Figs. 3 and 4.

The experiments can be divided into two categories: The first type of experiments with only one adsorption cycle (runs 1-6 of Table 2, Fig. 3(a)-(f)), and the second type with three cycles, i.e., two adsorption and one desorption, (runs 7-9 of Table 2, Fig. 4(a)-(c)). In fact, the second adsorption cycle was formed due to the

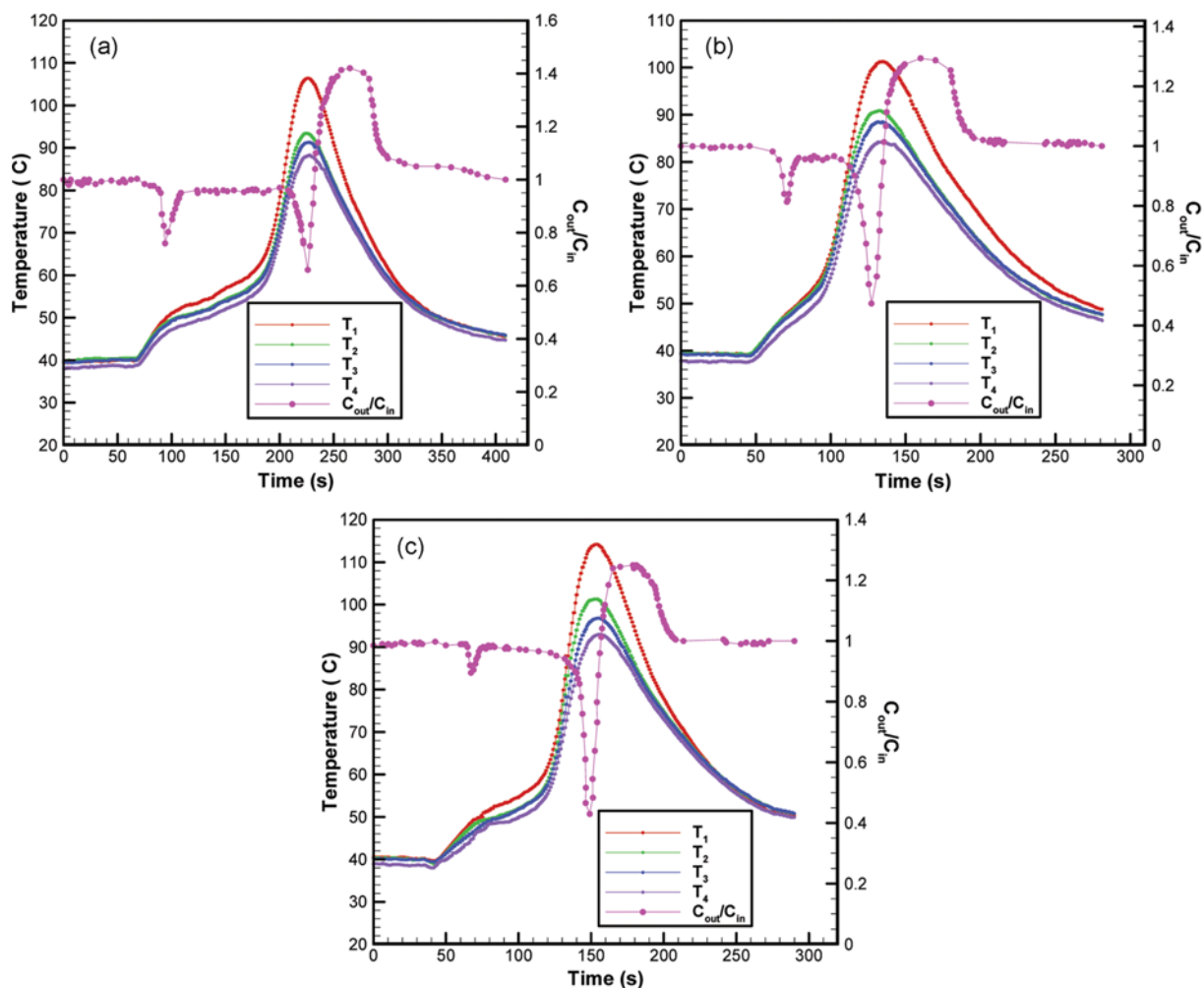


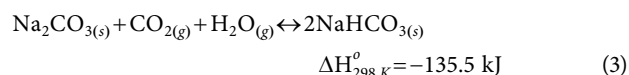
Fig. 4. The result of runs 7-9 of Table 2.

increase in the inlet temperature of the fluidized bed reactor up to 40 °C. These results indicate that the reaction mechanism depends on temperature. The reaction mechanism at different temperatures has been described in the section 3.4. (XRD results analysis), completely. Further proof on temperature dependence of the reaction can be found in the study by Siriwardane et al. [30]. They employed novel regenerable sodium-based sorbents for CO₂ capture. A new sorbent containing NaOH/CaO was used for CO₂ capture at a wide range of temperatures (from ambient temperature to 500 °C). The amount of adsorbed CO₂ at room temperature and 315 °C was approximately 3 and 2.5 mol of CO₂ per kg of the sorbent, respectively. That means the sorbent has an acceptable CO₂ sorption capacity at room temperature, but its capacity is different at higher temperatures.

3. Desorption Analysis

Fig. 4(a)-(c) shows that during the tests with two adsorption cycles (run 7-9 in Table 2), CO₂ desorption occurred in the temperature range of 90-115 °C. The possible reactions and their temperature ranges were investigated to assess the cause of CO₂ desorption in these experiments. In addition to carbonation reactions (1) and (2), which happen at ambient temperature, occurrence of reactions (3) and (4) with the sodium-based sorbents is also possi-

ble. CO₂ sorption can be achieved by Na₂CO₃, according to the following reaction [26]:



Reaction (3) occurs at 50 °C while NaHCO₃ decomposition (reaction (3-reverse)) proceeds at above 80 °C and completes in the range of 100-180 °C. With increasing temperature, NaHCO₃ converts to Na₂CO₃.

Depending on the chosen CO₂ sorbent, i.e. NaOH or Na₂CO₃, the cycle can be closed by either NaHCO₃ decomposition (reaction (3-reverse)) or Na₂CO₃ decomposition (reaction (4)) [26]:



Na₂CO₃ decomposition occurs at above 1,600 °C and proceeds in two steps, but discussion of these high temperature decompositions is totally beyond the scope of this paper [26,31]. Therefore, reaction (3-reverse) can take place in the temperature range of 90-115 °C and transformation of NaHCO₃ to Na₂CO₃ is the main reason for CO₂ desorption in some of experiments (run 7-9 in Table 2, Fig. 4(a)-(c)).

4. XRD Results Analysis

As mentioned earlier, the results are divided into two categories: The first group had only one adsorption cycle, and the second group had two adsorption and one desorption cycle. Characteristics of the fresh sorbents, the sorbent used in run 1 in Table 2 (as the representative of the first group of experiments) and the sorbent used in run 9 in Table 2 (as the representative of the second group) are shown in Fig. 2(a) to (c), respectively.

The XRD analysis of the fresh sorbent is displayed in Fig. 2(a), where the presence of sodium hydroxide is indicated by the stars. The XRD analysis of the reactor outflow during run 1 of Table 2 is depicted in Fig. 2(b). As can be seen, NaHCO₃ was formed in this run, which indicates that reaction (2) had happened. However, according to Fig. 2(c), which displays XRD analysis of the reactor outflow during run 9 of Table 2, Na₂CO₃ and NaHCO₃ were produced, which confirmed that reactions (1) and (2) had occurred. This could cause the second adsorption cycle in the experiments. These results indicate that the reaction mechanism depends on temperature. Based on Fig. 2 there is evidence that in both samples some of sorbent did not react with carbon dioxide, which illustrates the incomplete conversion of the sorbent.

Zhao et al. [32] stated that the most important issue in determining the suitability of an alkali metal for CO₂ capture is recognition of the carbonation reaction rate and CO₂ adsorption capacity of the sorbents. The most stable phase at low temperatures and high CO₂ pressures, is MHCO₃. Here, M represents alkali metals. When the temperature is increased, MHCO₃ is converted to M₂CO₃, which is stable over a wide range of pressures and temperatures.

5. The Optimal Conditions

The ratio of $\Delta C/\Delta t$ was selected as the optimization criterion. ΔC is the difference between CO₂ concentrations at the input and output of the reactor and Δt is the time needed for the gas flow to pass through the reactor. In fact, $\Delta C/\Delta t$ is same as CO₂ removal rate. Eq. (7) was used to compute CO₂ removal rate [7]:

$$\Delta C/\Delta t = \frac{\text{initial CO}_2 \text{ concentration} - \text{final CO}_2 \text{ concentration}}{t_{\text{initial}} - t_{\text{final}}} \quad (7)$$

where, the initial and final conditions are related to the beginning of the adsorption process and the minimum peaks (Fig. 3 and 4), respectively. Note that the absolute value of $\Delta C/\Delta t$ was calculated for all experiments, which is given in Table 2. Furthermore, $\Delta C/\Delta t$ (in ppm per second) is calculated and reported.

For experiments with two adsorption cycles, $\Delta C/\Delta t$ of the second cycle is reported. A larger $\Delta C/\Delta t$ is an indication of a greater concentration difference in a shorter period of time. Therefore, by comparing $\Delta C/\Delta t$ values of Table 2, run 1 was chosen as an optimal test. The amount of CO₂ captured by the sorbent was about 2.8 mol/kg. From analyzing the experimental data, $\Delta C/\Delta t$ had the maximum and minimum dependence on temperature and air flow rate, respectively. The results of the designed experiments and the effects of the operating parameters on $\Delta C/\Delta t$ are demonstrated in Fig. 5(a) to (c), which show that the conditions of run 1 of Table 2 resulted in the highest value of $\Delta C/\Delta t$ and run 1 is the optimal test.

6. The Effect of Operating Parameters

6-1. Temperature

Yi et al. [33] investigated the effect of reactor temperature on CO₂

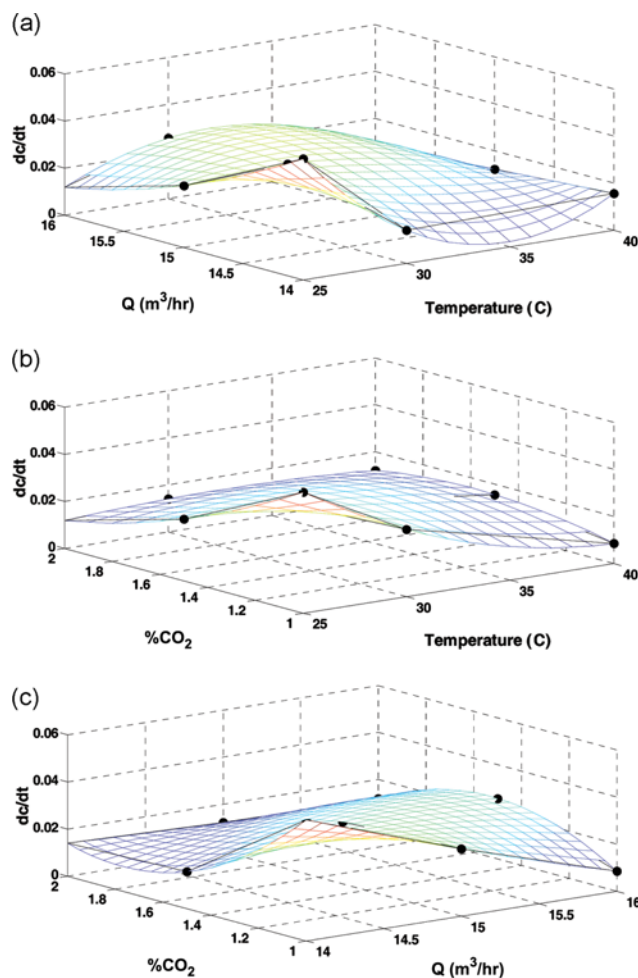


Fig. 5. The results of the designed experiments and the effect of the operating parameters on $\Delta C/\Delta t$ (a) temperature - air flow rate (b) temperature - CO₂ volume percentage (c) air flow rate - CO₂ volume percentage.

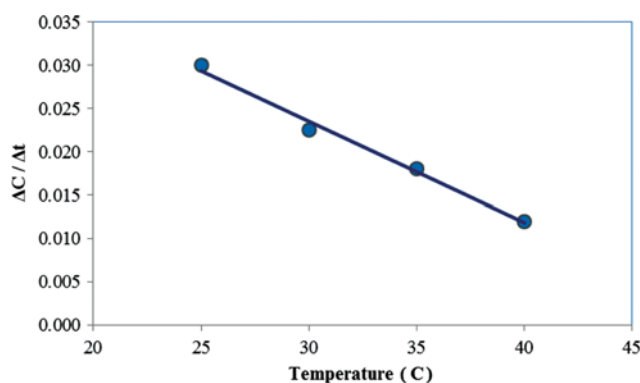


Fig. 6. The effect of temperature on $\Delta C/\Delta t$.

removal using NaHCO₃ sorbent in a fast fluidized bed reactor and reported that as the carbonation temperature was increased, the CO₂ removal decreased. According to Fig. 6, due to the exothermic nature of the reactions and the adsorption, $\Delta C/\Delta t$ decreased with increasing temperature. Since both carbonation reactions (1)

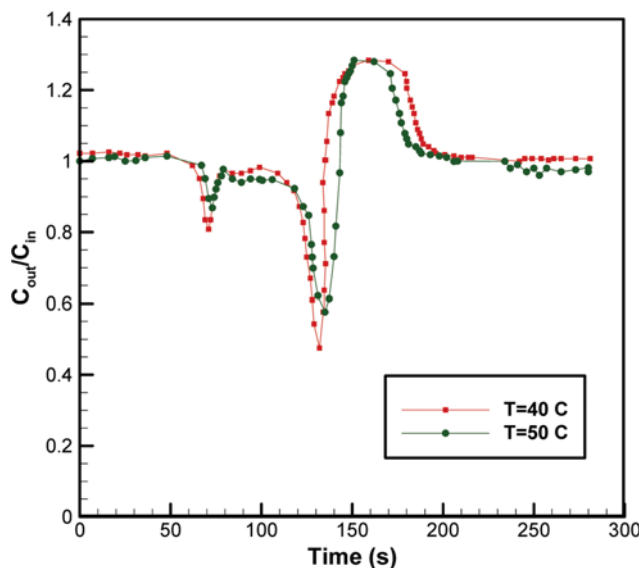


Fig. 7. The effect of temperature increment (CO_2 volume percentage of 1.5% and air flow rate of $14 \text{ m}^3/\text{hr}$).

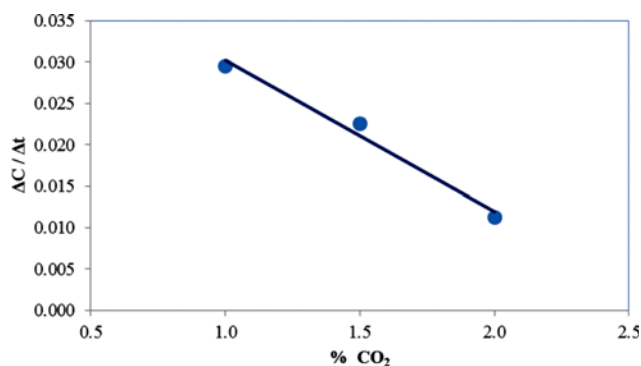


Fig. 8. The effect of CO_2 volume percentage on $\Delta C/\Delta t$.

and (2) are thermodynamically favorable at ambient temperature, a lower temperature is desirable to achieve a higher adsorption rate. To perform further investigation, two tests were conducted under specific conditions (CO_2 volume percentage of 1.5%, air flow rate of $14 \text{ m}^3/\text{hr}$, at 50 and 40°C). Fig. 7 shows that by increasing temperature to 50°C , $\Delta C/\Delta t$ was reduced. This finding confirms the negative effect of temperature increment.

6-2. CO_2 Volume Percentage

The effect of CO_2 volume percentage on $\Delta C/\Delta t$ is shown in Fig. 8, indicating that a higher inlet CO_2 volume percentage causes a reduction in $\Delta C/\Delta t$. Both sorbent and carbon dioxide are the reactants, so when the inlet CO_2 volume percentage is increased the sorbent cannot adsorb some of the excessive carbon dioxide.

6-3. Air Flow Rate

Yi et al. [33,34] investigated the effect of gas velocity on CO_2 removal using NaHCO_3 sorbent in a fast fluidized bed reactor and reported that the CO_2 removal decreases as the gas velocity is increased due to the reduction in contact time between the sorbent and the gas. They also repeated this study using K_2CO_3 sorbent and reached the same conclusion. In the present work, the effect

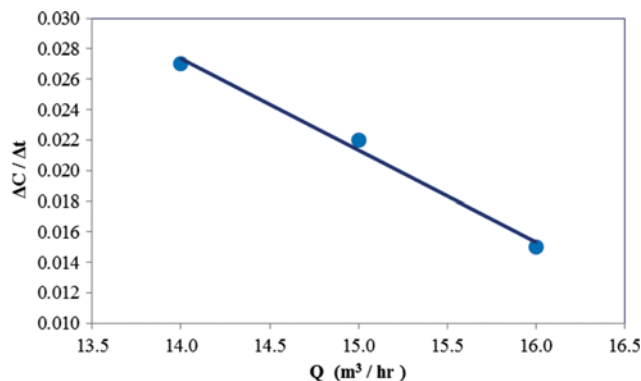


Fig. 9. The effect of air flow rate on $\Delta C/\Delta t$.

of air flow rate on $\Delta C/\Delta t$ is depicted in Fig. 9. As can be seen, a high inlet air flow rate leads to a reduction in $\Delta C/\Delta t$. This is due to the shorter gas-solid contact time at higher flow rates.

CONCLUSION

CO_2 capture using NaOH solid sorbent in a fluidized bed has been investigated experimentally. The impact of operating parameters, i.e., temperature, CO_2 volume percentage, and the inlet air flow rate on $\Delta C/\Delta t$ in the adsorption region, was carefully examined over time. The results indicate that increasing each of three operating parameters has a negative effect on $\Delta C/\Delta t$, and temperature is the most effective one. The results revealed the optimum value of $\Delta C/\Delta t$ ratio in the adsorption region is equal to $0.0515 (\%/s)$ ($515.277 (\text{ppm}/s)$). This value was achieved at a temperature of 25°C , CO_2 volume percentage at the inlet of 1% and the inlet air flow rate of $14 \text{ m}^3/\text{hr}$. The amount of CO_2 captured by the sorbent was about $2.8 \text{ mol}/\text{kg}$. In addition, the involved reactions were temperature-dependent. Consequently, only one adsorption cycle was observed at low temperatures ($25\text{--}30^\circ\text{C}$). As the temperature increased, the second adsorption cycle occurred and, finally, CO_2 desorption cycle took place in the range of $90\text{--}115^\circ\text{C}$. Furthermore, when sodium hydroxide hold-up was 0.1 kg , the inlet temperature and inlet air flow rate were in the ranges of $25\text{--}30^\circ\text{C}$ and $14\text{--}16 \text{ m}^3/\text{hr}$, respectively.

REFERENCES

1. D. M. Kim and J. Cho, *Korean J. Chem. Eng.*, **28**, 22 (2011).
2. A. Benamor and M. K. Aroua, *Korean J. Chem. Eng.*, **24**, 16 (2007).
3. F. Karadas, M. Atilhan and S. Aparicio, *Energy Fuels*, **24**, 5817 (2010).
4. H. Yang, Z. Xu, M. Fan, R. Gupta, R. Slimane and A. Bland, *J. Environ. Sci.*, **20**, 14 (2008).
5. M. Duke, B. Ladewig, S. Smart, V. Rudolph and J.D. d. Costa, *Front. Chem. Sci. Eng.*, **4**, 184 (2010).
6. B. Dutcher, M. Fan and B. Leonard, *Sep. Purif. Technol.*, **80**, 364 (2011).
7. M. Kianpour, M. Sobati and S. Shahhosseini, *Chem. Eng. Res. Des.*, **90**, 2041 (2012).
8. K. Kim, D. Kim, Y.-K. Park and K. S. Lee, *Int. J. Greenhouse Gas*

- Control*, **26**, 135 (2014).
9. T. Gupta and R. Ghosh, *Int. J. Greenhouse Gas Control*, **32**, 172 (2015).
 10. M. M. Shahrestani and A. Rahimi, *Environ. Eng. Res.*, **19**, 299 (2014).
 11. M. G. Plaza, I. Durán, F. Rubiera and C. Pevida, *Appl. Energy*, **144**, 182 (2015).
 12. M. Alfea, P. Ammendola, V. Gargiulo, F. Raganatib and R. Chirone, *Proceedings of the Combustion Institute*, **35**, 2801 (2015).
 13. H. Seo, D. Y. Min, N. Y. Kang, W. C. Choi, S. Park, Y.-K. Park and D. K. Lee, *Korean J. Chem. Eng.*, **32**, 51 (2015).
 14. V. Nikulshina, C. Gebald and A. Steinfeld, *Chem. Eng. J.*, **146**, 244 (2009).
 15. J. W. Butler, C. J. Lim and J. R. Grace, *Chem. Eng. Res. Des.*, **89**, 1794 (2011).
 16. M. S. Masnadi, J. R. Grace, X. T. Bi, N. Ellis, C. J. Lim and J. W. Butler, *Energy*, **83**, 326 (2015).
 17. J. Blamey, V. Manovic, E. J. Anthony, D. R. Dugwell and P. S. Fennell, *Fuel*, **150**, 269 (2015).
 18. S. Pourebrahimi, M. Kazemeini, E. G. Babakhani and A. Taheri, *Micropor. Mesopor. Mater.*, **218**, 144 (2015).
 19. D. Cheng, Y. Liu, H. Wang, X. Weng and Z. Wu, *J. Environ. Sci.*, **38**, 1 (2015).
 20. G. Duelli, A. Charitos, M. E. Diego, E. Stavroulakis, H. Dieter and G. Scheffknecht, *Int. J. Greenhouse Gas Control*, **33**, 103 (2015).
 21. A. Antzara, E. Heracleous and A. A. Lemonidou, *Appl. Energy*, **156**, 331 (2015).
 22. D. Kunii and O. Levenspiel, *Fluidization engineering*, 2nd Ed., Butterworth-Heinemann, Boston (1991).
 23. M. Ayobi, S. Shahhosseini and Y. Behjat, *J. Taiwan. Inst. Chem. E.*, **45**, 421 (2013).
 24. J.-H. Choi, C.-K. Yi, S.-H. Jo, H.-J. Ryu and Y.-C. Park, *Korean J. Chem. Eng.*, **31**, 194 (2014).
 25. W. Zhang, H. Liu, C. Sun, T. C. Drage and C. E. Snape, *Chem. Eng. Sci.*, **116**, 306 (2014).
 26. V. Nikulshina, N. Ayesa, M. E. Galvez and A. Steinfeld, *Chem. Eng. J.*, **140**, 62 (2008).
 27. Cameron-cole, *Salt creek phases III/IV environmental assessment*, U.S. Department of the Interior (2006).
 28. J. B. Lee, C. K. Ryu, J.-I. Baek, J. H. Lee, T. H. Eom and S. H. Kim, *Ind. Eng. Chem. Res.*, **47**, 4465 (2008).
 29. D. Geldart, *Powder Technol.*, **7**, 285 (1973).
 30. R. V. Siriwardane, C. Robinson, M. Shen and T. Simonyi, *Energy Fuels*, **21**, 2088 (2007).
 31. Y. Liang, *Carbon dioxide capture from flue gas using regenerable sodium-based sorbents*, Master of Science in Chemical Engineering, Tsinghua University, Beijing, China (2003).
 32. C. Zhao, X. Chen, E. J. Anthony, X. Jiang, L. Duan and Y. Wu, *Prog. Energy Combust. Sci.*, **39**, 515 (2013).
 33. C.-K. Yi, S. H. Jo, Y. Seo, S. D. Park, K. H. Moon and J. S. Yoo, *Stud. Surf. Sci. Catal.*, **159**, 501 (2006).
 34. C.-K. Yi, S.-H. Jo, Y. Seo, J.-B. Lee and C.-K. Ryu, *Int. J. Greenhouse Gas Control*, **1**, 31 (2007).